# Characterization of biochemical changes associated with TCDD exposure in the cellular secretions of *in vitro* endometriosis models via Raman spectroscopy-based measurements

By

Jeremiah J. Johnson

Thesis

Submitted to the Faculty of the

Graduate School of Vanderbilt University

In partial fulfillment of the requirements

for the degree of

MASTER OF SCIENCE

in

Biomedical Engineering

August 11, 2023

Nashville, Tennessee

Approved:

Andrea Locke, Ph.D.

Kaylon Bruner-Tran, Ph.D.

## *ACKNOWLEDGEMENTS*

I would like to thank our collaborators at the Women's Reproductive Health Research Center at Vanderbilt University Medical Center as well as Dr. Bruner-Tran and Dr. Osteen. Such efforts could not have been made possible without their contributions.

I would also like to thank the members of the Locke Biosensing Lab for their continual assistance and guidance throughout my brief tenure as a graduate student. Additionally, thank you to everyone involved with the Vanderbilt Biophotonics Center for all their support and for creating such a welcoming environment for me to learn. Special shout out to Dr. Locke for taking me in as a dual-degree student and teaching me the fundamentals of Raman spectroscopy.

Lastly, I would like to thank my family for their never-ending love and understanding, especially throughout this past year. Mom, Dad, Javante, and Serena, I appreciate you all more than you can ever know.

# Table of Contents

Page

***ACKNOWLEDGEMENTS*** ..... ii

***LIST OF FIGURES*** ..... v

***LIST OF TABLES*** ..... vi

Chapter

**I** ***INTRODUCTION AND BACKGROUND*** ..... 1

Endometrium Biology ..... 1

Endometriosis ..... 2

*Pathogenesis and Pathophysiology* ..... 3

*Symptomology and Disease Progression* ..... 4

*Risk Factors and Treatments* ..... 5

*Current Diagnostic Methods* ..... 6

*Novel Technologies for Diagnosis* ..... 8

Raman Spectroscopy ..... 10

*Applications of Raman Spectroscopy for Diagnostic Purposes* ..... 13

Research Objectives ..... 14

References ..... 15

**II** ***IN VITRO INVESTIGATION OF ENDOMETRIOSIS MODELS VIA RAMAN-BASED MEASUREMENTS*** ..... 24

Specific Aims ..... 24

Introduction ..... 26

Methods ..... 28

*Sample Collection* ..... 28

*Drop-Cast Raman Measurement Protocol* ..... 30

*Raman Data Processing* ..... 32

*Raman Spectral Analysis* ..... 32
Results ..... 34
*Optimizing Raman Spectroscopy Measurement Parameters* ..... 34
*Spectral Peak Detection* ..... 34
*Raman Data Analysis* ..... 38
Discussion ..... 40
References ..... 43
**III *CONCLUSIONS AND FUTURE DIRECTIONS*** ..... 46
References ..... 49

# *LIST OF FIGURES*

Page

**Figure 1.** H&E staining of endometrial tissue ..... 1

**Figure 2.** Reproductive tract of endometriosis patient ..... 3

**Figure 3**. H&E staining of endometriotic lesion at 100x magnification ..... 3

**Figure 4.** Non-laparoscopic diagnostic methods for endometriosis ..... 7

**Figure 5.** Tunable fluorescence imaging ..... 10

**Figure 6.** Modes of scattering. ..... 11

**Figure 7.** Cell collection and treatment process ..... 29

**Figure 8.** Triplicate droplet technique ..... 30

**Figure 9.** Raman spectral processing ..... 32

**Figure 10.** Example of averaged Raman spectra ..... 33

**Figure 11**. Raman spectra of murine bone marrow-derived macrophages ..... 35

**Figure 12.** Raman spectra of human endometrial stromal cells ..... 36

**Figure 13.** PCA plots for murine bone marrow-derived macrophages ..... 38

**Figure 14.** PCA plots for human endometrial stromal cells ..... 39

**Figure 15.** Inter-sample PCA plots between human endometrial stromal cells and murine bone marrow-derived macrophages ..... 40

**Figure 16.** CAD model for glass slide holder ..... 47

**Figure 17.** Glass slide holder dimensions ..... 47

# *LIST OF TABLES*

Page

**Table 1.** Revised American Society for Reproductive Medicine staging system ..... 5

**Table 2.** CA-125 biomarker for endometriosis detection..... 9

**Table 3.** Experimental sample dataset..... 28

**Table 4.** Raman peak correlation table..... 37

# *CHAPTER I: INTRODUCTION AND BACKGROUND*

## Endometrium Biology

The endometrium is the mucosal tissue that lines the uterine cavity. Its primary function is to provide a stable, nourishing environment for embryonic implantation and fetal development. The endometrium consists of two distinct layers: stratum basalis and stratum functionalis (Fig. 1). Both regions are vascularized and reside medial to the myometrium.[1]

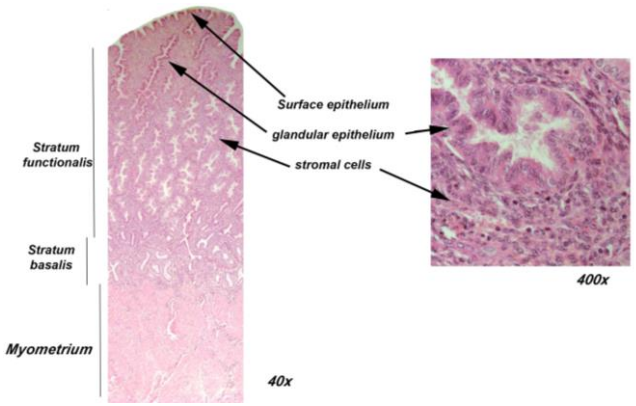


**Figure 1.** H&E staining of endometrial tissue. Left: 40x magnification; Right: 400x magnification.

The stratum basalis or basal layer lies adjacent to the smooth muscle of the uterus (i.e. myometrium) and serves to sufficiently secure the endometrium within the uterine cavity. The growth and maintenance of the stratum basalis is largely independent of hormonal fluctuations throughout the menstrual cycle. Furthermore, stem cells within this region enable the regeneration of the stratum functionalis. The stratum functionalis or functional layer is primarily comprised of specialized stromal cells and epithelial cells (e.g., surface and glandular). This layer also contains endothelial cells that form a network of blood vessels that traverse the tissue. Unlike the basal layer, growth and differentiations of the functional layer are highly regulated by steroid hormone concentrations. The characteristic cyclical proliferative and menstrual phases of the reproductive-age women is attributed to the estrogen- and progesterone-dependent stimulation of the stratum functionalis. Additionally, the immune cell populations within the endometrium fluctuate throughout the menstrual cycle in response to hormonal changes.[1,2]

The typical menstrual cycle ranges between 25 and 35 days and contains distinct stages that are regulated by steroids.[3,4] The phases of the menstrual cycle are the menstrual, proliferative, and the secretory phases.[5] Menstruation is characterized by the shedding of the endometrium, specifically, the stratum functionalis. During this phase, most women experience blood expulsion through the vaginal cavity that typically lasts between three and seven days. The proliferative phase consists of high rates of endometrial cell division/proliferation in response to increased estrogen concentrations. This results in endometrial thickening prior to ovulation. Lastly, the secretory phase is dominated by progesterone and, to a lesser extent, estrogen. These hormones promote endometrial differentiation in preparation for embryonic implantation. In the absence of pregnancy, the corpus luteum degrades, hormone concentrations dramatically decrease, the onset of menstruation occurs, and the cycle repeats.[5]

As previously mentioned, the menstrual cycle occurs about once every month in the absence of pregnancy. Menstrual cycles first begin shortly after the onset of puberty, become irregular with the onset of menopause, then eventually cease. For most biological females, these milestones occur around the ages 13 and 51, respectively. In the absence of disease, pregnancy, or steroidal contraception, most women can expect to experience more than 450 menstrual cycles across their reproductive lifespan.[5,6] However, conditions that disrupt the endocrine and/or immune systems are capable of impeding endometrial function and reducing fertility.[7]

**Endometriosis**

Endometriosis is a chronic gynecological disease that affects approximately 10-12% of reproductive-age women (more than 190 million worldwide). It is characterized by the presence of endometrial tissue outside, or ectopic, of the uterine cavity, which – similarly to the intrauterine, or eutopic, endometrium – undergoes periods of proliferation and deterioration in

response to fluctuations in estrogen and progesterone levels (Fig. 2).[8] Endometriosis can be exceptionally difficult to detect. In fact, many women experience a 7–10-year delay before a definitive diagnosis. Such delays coupled with the limited effectiveness of current treatment options are often associated with disease progression and can have a detrimental impact on reproductive health. For poorly understood reasons, the global prevalence of endometriosis has steadily increased since 2009.[9]

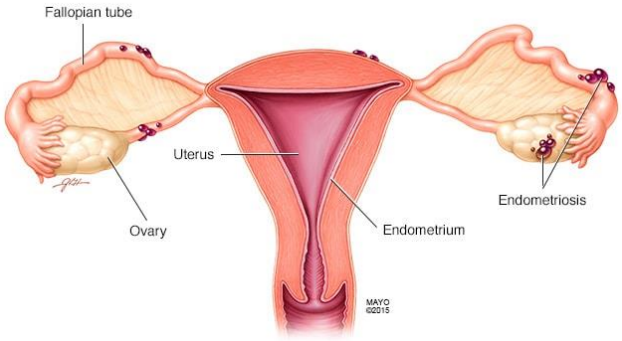


**Figure 2.** Reproductive tract of endometriosis patient.[8] *Used with the permission of Mayo Foundation for Medical Education and Research, all rights reserved.*

***Pathogenesis and Pathophysiology***

As aforementioned, endometriosis is defined by the abnormal growth of endometrium-like tissue outside of the uterine cavity. Similar to the endometrium, these extra-uterine tissues consist of endometrial stromal and epithelial cells, as well as iron deposits (Fig. 3). Furthermore, the proliferation of the endometriotic lesions can coincide with the menstrual cycle in a manner similar to normal endometrial tissue; however, these tissues are often progesterone resistant.[10]

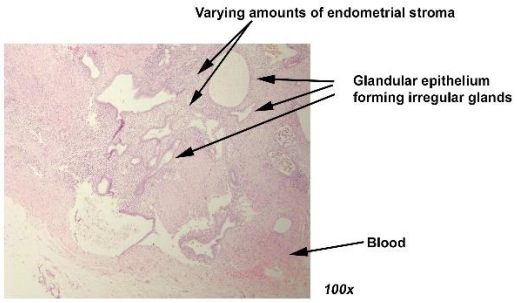


**Figure 3**. H&E staining of endometriotic lesion at 100x magnification.

Compared to many other chronic diseases, the pathogenesis of endometriosis is poorly understood. Currently, the prevailing theories regarding its etiology include retrograde menstruation, endometrial cell transport, Müllerian rests, and toxin- or hormone-induced cell

transformation.[8,10] Since the presentation of endometriosis can vary significantly across patients, most clinicians and scientists agree that there is not a singular overarching cause of disease.

***Symptomology and Disease Progression***

The symptomology and clinical manifestations of endometriosis vary widely from patient to patient, and as is the case with many chronic conditions, the effects of endometriosis are exacerbated in the absence of the appropriate treatment.

Although the precise pathogenesis of endometriosis is debated, the symptomology has been comprehensively defined. Upon the initial onset of symptoms, afflicted patients typically experience pelvic pain and discomfort during their menstrual period (i.e. dysmenorrhea). Intermediate symptoms include fatigue, excessive menstrual flow, and infertility. Patients with endometriosis who become pregnant are at increased risk of early pregnancy loss, preterm birth, and other complications.[59] Progression of endometriosis can eventually lead to bowel obstruction, fibrosis, and pelvic/intrauterine adhesions (IUA) which further compromise the patient's health and quality of life. [8,11]

Although poorly characterized relative to other chronic conditions, the American Society for Reproductive Medicine has implemented a standardized staging system for endometriosis. These stages range from 1 to 4 and are dictated by the quantity, size, and depth of endometriotic lesions (Table 1).[12] This approach is quite subjective but offers insight into disease progression and patient prognosis. However, the presence and characteristics of potential endometriotic lesions can only be confirmed via laparoscopy – an invasive surgical procedure.[13]

**Table 1.** Revised American Society for Reproductive Medicine staging system.[12]

| rASRM Stage | Alternative Name | Score | Manifestations of Endometriosis |
|---|---|---|---|
| Stage 1 | Minimal | 1-5 points | Few superficial growths |
| Stage 2 | Mild | 6-15 points | Some deep growths |
| Stage 3 | Moderate | 16-40 points | Many deep growths, small cyst(s), some adhesions present |
| Stage 4 | Severe | 40+ points | Many deep growths, large cyst(s), many deep adhesions |

***Risk Factors and Treatments***

There are several factors that increase the risk of developing endometriosis. These early menarche (i.e., before the age of 11), abnormal menstrual periods, chronically elevated estrogen levels, sustained damage to the reproductive tract, genetic predispositions, a family history of endometriosis, and prolonged exposure to toxic agents.[11,14,15] Environmental toxicants, such as 2,3,7,8-tetrachlorodibenzo-*p*-dioxin (TCDD), are commonly found in fires, cigarettes, and processed foods. TCDD is a known endocrine and immune disruptor, and thus, has often been suggested to play a role in the development of endometriosis.[16,60,61,62]

Although there is no current cure for endometriosis, there are several treatment options for disease management. Conservative approaches typically involve altered dietary habits and prescribed pain medications, such as nonsteroidal anti-inflammatory drugs (NSAIDs) and ibuprofen.[8,11,17] If symptoms do not improve, patients are treated with hormone therapy. This option includes hormonal contraceptives, gonadotropin-releasing hormone (Gn-RH) agonists and antagonists, and aromatase inhibitors. The purpose of these therapies is to artificially decrease estrogen concentrations, thus mitigating endometrial tissue growth and painful menstrual cycles.

However, hormone therapy can lead to many adverse complications such as mood swings, decreased bone density, and induction of a menopause-like state in patients. Additionally, such treatments are generally not viable for women seeking pregnancy. Surgical procedures are a last resort and typically reserved for patients with severe cases of endometriosis (i.e., exceptional pain and/or high risk of intrauterine adhesions).[17]

***Current Diagnostic Methods***

As stated earlier, most patients with endometriosis will suffer for ten years or more after disease onset before being properly diagnosed.[18] A major reason for such delayed diagnoses is the lack of reliable biomarkers along with poor visibility of endometriomas using current imaging modalities. This has severely limited detection rates, resulting in uninhibited disease progression and suboptimal patient outcomes. The current diagnostic methods for endometriosis are pelvic examinations, ultrasound, magnetic resonance imaging (MRI), computed tomography (CT), and laparoscopy – the gold standard.[8,11,19] Outside of laparoscopic examinations, which are invasive surgical procedures, diagnostic sensitivity for endometriosis is often poor and varies based on the skill of the physicians.

Pelvic exams and imaging techniques have displayed poor negative predictive values and sensitivities when performed independently. A few studies have demonstrated the relative ineffectiveness of bimanual pelvic examinations and transvaginal sonograms. One particular group, found that out of 91 endometriosis-positive patients, 43 (47%) and 37 (41%) exhibited "unremarkable" pelvic exams and sonographic evaluations, respectively.[20] Furthermore, CT scans are largely ineffective for visualizing pelvic organs, and while MRI possesses greater sensitivity than ultrasound, it is expensive and requires specialized medical equipment.[21] Overall,

these diagnostic techniques often yield inconclusive results that must be confirmed via laparoscopy (Fig. 4).

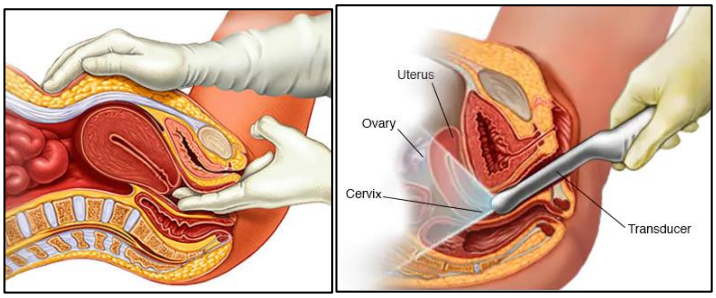


**Figure 4.** Non-laparoscopic diagnostic methods for endometriosis. Pelvic examination (left); transvaginal ultrasound (right).[8] *Used with the permission of Mayo Foundation for Medical Education and Research, all rights reserved.*

Despite being the current gold standard, laparoscopic procedures still present many challenges. Inherent constraints such as limited vision and range of motion, poor depth perception, the need for highly trained surgeons, and disproportionate access to quality healthcare, impair the diagnostic effectiveness of laparoscopy.[22] Additionally, this technique possesses quite a low specificity (40%) due to the exclusive reliance on the peritoneal lesion visualization.[23] In 2021, a meta-analysis study reported that nearly half of all positive laparoscopic surgeries for endometriosis were later deemed incorrect diagnoses.[24] This indicates that surgeons mistakenly attribute the peritoneal lesions they identify during laparoscopy to endometriosis instead of the actual causes: acute inflammation, hemangiomas, hemosiderin deposits, and mesothelial hyperplasia.[25] Tissue resections and biopsies (i.e. histopathology) greatly improve specificity and negative predictive values but require additional time and resources.[26] Furthermore, the risks of peritoneal perforations, excessive bleeding, sepsis, anesthesia-related reactions, and other adverse complications discourage patients from explorative laparoscopy until symptoms progress.[27]

The current landscape of diagnostic techniques for endometriosis is inadequate and underwhelming. More specifically, the lack of effective, non-invasive diagnostic approaches is

contributing to the high rates of delayed diagnoses and disease progression in millions of reproductive-age women.

### *Novel Technologies for Diagnosis*

The shortcomings of current diagnostic tools have sparked novel developments for endometriosis detection. From gene profiling and omics approaches to spectroscopic analyses, significant strides are being made to bolster the effectiveness of non-invasive diagnostic tools for endometriosis.

**Serum Biomarkers.** As previously mentioned, there are currently no validated biomarkers for endometriosis. However, several studies have explored the biomolecular profile associated with disease progression.[28,29,30] Such indicators include glycoproteins, chemokines, inflammatory cytokines, angiogenic factors, and micro RNAs (miRNAs). Specifically, vascular endothelial growth factor (VEGF), urocortin (UCN), cancer antigen-125 (CA-125), and cancer antigen-19-9 (CA-19-9) are of interest. These have been researched with widely variable and inconsistent results, rendering clinical effectiveness inconclusive. For example, the sensitivities and specificities of five studies primarily focused on CA-125 for diagnosis of early-stage endometriosis (i.e. Stage I-II) ranged from 50-92.3% and 71-72%, respectively.[31,32,33,34,35] Generally, immunoassays (i.e. radioimmunoassays, immunofluorescence assays, enzyme-linked immunosorbent assays [ELISAs], etc.) are used to accurately measure antigen concentrations in serum samples.[36]

Omics is a quickly rising field of study comprising proteomics, metabolomics, transcriptomics, and genomics. This technology refers to the comprehensive study of all biomolecular substances and/or processes. Although promising studies (with unstandardized

methodologies) have exhibited remarkable sensitivities and specificities, this technique is exceptionally costly and time intensive.[37,38,39,40,41]

Using immunoassays and gene/proteomic profiling techniques, researchers have displayed diagnostic sensitivities comparable to laparoscopy without histology (Table 2). However, long preparation times (i.e., sufficient labeling and equipment setup) and the need for expensive materials paired with discrepancies across research groups, have prevented widespread clinical adoption.[42]

**Table 2.** CA-125 biomarker for endometriosis detection.[30,31,32,33,34]

| **Biomarkers** | **Sample Size** | **Sensitivity (%)** | **Specificity (%)** | **Reference** |
|---|---|---|---|---|
| CA-125 | 38 | 92.3 | 72 | Xavier, 2005 |
| CA-125 | 231 | 55.8 | 92.8 | Cho, 2008 |
| CA-125 | 23 studies | 50 | 72 | Mol, 1998 |
| CA-125 | 685 | 76 | 71 | Cheng, 2002 |
| CA-125+IL-8+TNF-α | 294 | 89.7 | 71.1 | Mihalyi, 2010 |

**Optical Techniques.** Optical techniques rely on the interactions between incident light and a material of interest to determine its physical, chemical, or structural properties. Within diagnostic contexts, these approaches provide real-time analysis in a non-invasive manner. Methods such as fluoroscopy and attenuated total reflection infrared spectroscopy (ATR-IR) have been utilized in studies to diagnose endometriosis.

Fluoroscopy is an imaging modality that uses continuous x-ray beams to create images of patient tissues. It is a minimally invasive technique based on the principle of fluorescence.[43] This method is often paired with indocyanine green, a non-toxic dye, for enhanced contrast and visualization of neovascularization, which has been linked to endometriosis (Fig. 5).[44]

ATR-IR is a sampling approach that synergistically combines the principles of total internal reflection and infrared spectroscopy in order to assess a material's biochemical characteristics. Since the resultant evanescent waves have limited range, samples must be in direct contact with the ATR crystal. The characteristic IR absorption spectra produced enables distinctions between different biomolecules. A 2019 study demonstrated the ability of IR spectroscopy to detect biochemical changes in granulosa cells from patients with endometriosis. They reported that alterations to protein, lipid, and carbohydrate profiles were detected using IR spectroscopy. Specifically, the amount of phosphorylated proteins increased significantly while the amount of carbohydrates and RNA decreased significantly relative to the control as measured by IR spectroscopy.[46] Although promising, the need for direct contact can potentially damage biological samples and limits the sample type and size.

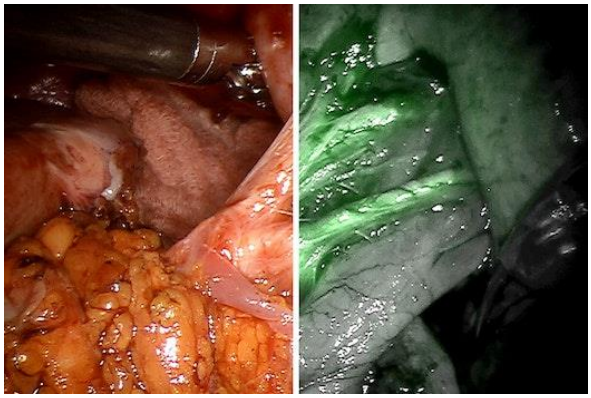

**Figure 5.** Tunable fluorescence imaging. Normal endoscopic view (left); indocyanine green-mediated fluoroscopy view (right).[45] *Copyright © 2023 Intuitive Surgical Operations, Inc.*

Despite the numerous advancements to improve diagnostic capabilities for endometriosis, none have been validated for clinical diagnosis. Therefore, there is still a significant need for a novel diagnostic tool to detect early-stage endometriosis in a non-invasive manner with minimal sample preparation and limitations to the sample type.

**Raman Spectroscopy**

Similar to IR spectroscopy, Raman spectroscopy (RS) is an analytical technique based on the interactions between light and a sample of interest. However, RS relies on the characteristic

inelastic scattering induced by the vibrational modes of molecular structures and chemical bonds during photonic collisions. The degree of inelastic scattering is known as the Raman shift and provides specific information pertaining to the chemical, structural, and physical properties of a sample. Such a non-invasive optical technique allows for the rapid, accurate, and label-free identification of macromolecular compounds with minimal damage to the observed specimen. Raman spectroscopy is a powerful tool, and its resultant unique spectral peaks enable effective analysis across a wide array of applications.[47]

Within the small particle regime, there are two primary types of scattering: elastic and inelastic. Elastic scattering or Rayleigh scattering refers to a scattering event between photons and particles that results in no gain or loss in energy (i.e., no change in photon wavelength). On the other hand, a change in photon energy and wavelength occurs during Raman scattering. There are two primary subtypes of Raman scattering: Stokes and anti-Stokes. In Stokes scattering, there is a resultant decrease in energy, in that the emergent wavelength of light is greater than the incident wavelength. Anti-Stokes scattering results in an increase in energy, in that the emergent wavelength of light is less than the incident wavelength. For both Rayleigh and Raman scattering, molecules are transiently excited to a virtual energy state upon their collision with incident photons.[48] The wavelength of the emergent light upon molecular relaxation dictates the type of scattering, as previously mentioned (Fig. 6).

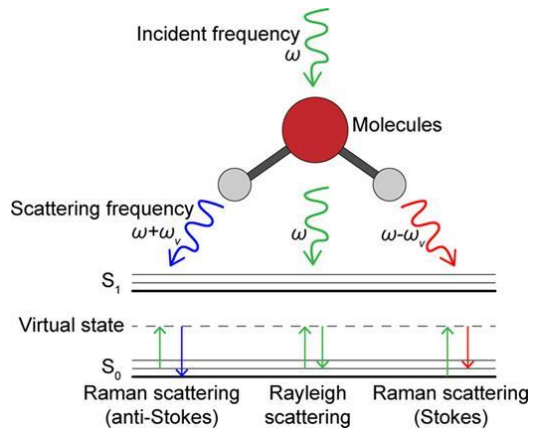


**Figure 6.** Modes of scattering.[49] *Reprinted from Lin et al., 2021, with the permission of AIP Publishing.*

Although an effective analytical technique, RS is not without its limitations. The primary shortcoming is the inherent inefficiency of Raman scattering. Only an approximate 1 in every $10^6$ –$10^8$ photons of an incident light beam will undergo inelastic scattering and produce a Raman signal.[48,51] Light-matter interactions are dominated by absorption, followed by subsequent fluorescence, and elastic scattering. Therefore, it can be difficult to obtain a sufficient Raman signal without high laser powers or prolonged exposure times, which can damage biological specimens. Additionally, the dominating presence of autofluorescence background within the spectral measurements necessitates advanced extraction methods to isolate the desired Raman signal and improve the signal-to-noise ratio (SNR).[50]

Several efforts have been made to circumvent the aforementioned limitations of RS. For example, the principle of surface plasmon resonance (SPR) is universally employed to improve signal intensity. The SPR effect is a phenomenon that enhances the electromagnetic (EM) response via the collective oscillation of conduction band electrons in resonance with the electric field of an incident light beam. The EM augmentation occurs at the surface of plasmonic substrates and is largely dependent on both the intensity of the incident electric field as well as the substrate's polarizability, as exemplified by the equation $\mu = \alpha * E$ (where $\mu$ is dipole moment, $\alpha$ is polarizability, and E is electric field).[51] Materials such as gold, silver, copper, and aluminum possess a negative real permittivity – which facilitates the SPR effect – have been used to boost Raman scattering efficiency up to $10^{14}$-fold.[52] Additionally, the researchers have addressed Raman spectroscopy's spectral analysis issue. Several techniques have been developed to eliminate extraneous background noise while retaining Raman signal. Many of these processing methods utilize a combination of smoothing filters, polynomial background subtraction, and spectral normalization to combat poor SNR and enable comparison between spectra.[50]

### *Applications of Raman Spectroscopy for Diagnostic Purposes*

The characteristic spectral peaks generated by Raman spectroscopy coupled with minimal sample preparation have made it a viable analytical tool for biomedical applications. The prevalence of RS within the medical realm has increased significantly, particularly for diagnostic purposes.

Numerous studies have demonstrated the potential of RS as a viable technique for efficient, non-invasive detection of disease-related biomarkers and quantification of pathophysiological responses. RS has been used for a broad array of applications within *in vivo*, *ex vivo*, and *in vitro* settings. From cancers to chronic conditions, such as diabetes and osteoarthritis, to malaria, RS has enabled effective detection and classification across several classes of disease.[53] One study reported the ability to distinguish between bronchial tissue specimens (n = 28; 12 normal, 10 squamous cell carcinoma [SCC], and 6 adenocarcinoma) using a 785nm RS excitation laser with 94% sensitivity and 94% specificity.[54] Furthermore, an *ex vivo* study on resected tumor samples of 34 patients with non-small cell lung cancer demonstrated the ability of RS to predict early postoperative cancer recurrence with a 73% sensitivity and 74% specificity.[55]

In recent years, RS has been employed to characterize endometriotic cells in a non-destructive and label-free manner. A 2019 study, using 94 blood serum samples (49 endometriosis patients; 45 control/healthy individuals) reported the creation of an algorithm that relies on RS measurements to diagnose endometriosis. The model yielded a sensitivity of 80.5% and a specificity of 89.7% within the training set (80 samples). Furthermore, the model exhibited high sensitivity and specificity (i.e. 100%) for the test set (14 samples; 8 endometriosis patients; 6 control).[56] Additionally, a study published in 2022 utilized RS to garner insight into the disease

progression of endometriosis. Using blood serum samples from 100 subjects (50 healthy women; 50 women with endometriosis), the group reported distinctions between the control and endometriotic Raman spectra. Significant shifts in peaks were identified. These shifts were attributed to chemical and structural alterations in functional groups following the onset of endometriosis. The results also exemplified a positive correlation between endometrioma volume lipid peak intensity.[57] Although promising, there are very few RS-related studies for the detection of endometriosis which exemplifies the need for further research before clinical implementation.

Raman spectroscopy is a power tool capable of accurately assessing subtle biomolecular differences between healthy and diseased patients for non-invasive and label-free diagnosis.

**Research Objectives**

The goal of this study was to characterize the biochemical changes induced by 2,3,7,8-tetrachlorodibenzo-*p*-dioxin (TCDD) using *in vitro* models via Raman-based measurements. The secretions of both murine and human cells were evaluated and compared to control models in order to determine the effects of TCDD-exposure on metabolic *in vitro* processes. As aforementioned, TCDD is believed to promote the development of endometriosis in humans and has been demonstrated to induce an endometriosis-like phenotype in mice.[58] In our research, TCDD exposure was used to induce metabolic changes to mimic endometriosis. Furthermore, in order to differentiate between the biochemical responses of cells with the endometriosis phenotype and cells merely experiencing acute inflammation, lipopolysaccharide (LPS), a common proinflammatory molecule, will serve as the positive control. By measuring and analyzing the Raman spectra produced from the cellular secretions of our *in vitro* samples, we

seek to discover characteristic molecular biomarkers for more effective early-stage detection of endometriosis.

**Primary Goal:** Utilize Raman-based measurements to monitor the biochemical changes induced in the cellular secretions of *in vitro* murine and human models following exposure to TCDD.

## References


1. Ochoa Marieta C, Barranquero Gómez M, Dolz Arroyo M, Fabra Roca P, Collazos Robles R, Salvador Z. What is the endometrium? - Thickening, types and pathologies. Algarra Goosman C, ed. *inviTRA*. Published online November 30, 2021. https://www.invitra.com/en/endometrium/#composition-of-the-endometrium
2. Barbieri RL. The endocrinology of the menstrual cycle. *Methods Mol Biol*. 2014;1154:145-169. doi:10.1007/978-1-4939-0659-8_7
3. Rogel Cayetano S, Ferrando Gilabert N, Salvador Z. The Different Phases of the Menstrual Cycle. Packan R, ed. *inviTRA*. Published online January 14, 2020. https://www.invitra.com/en/phases-of-the-menstrual-cycle/
4. Mihm M, Gangooly S, Muttukrishna S. The normal menstrual cycle in women. *Anim Reprod Sci*. 2011;124(3-4):229-236. doi:10.1016/j.anireprosci.2010.08.030
5. Thiyagarajan DK. Physiology, Menstrual Cycle. StatPearls - NCBI Bookshelf. https://www.ncbi.nlm.nih.gov/books/NBK500020/. Published October 24, 2022.
6. Hall JE. Endocrinology of the Menopause. *Endocrinol Metab Clin North Am*. 2015;44(3):485-496. doi:10.1016/j.ecl.2015.05.010
7. Endometrial Hyperplasia. *Yale Medicine*. Published online February 23, 2023. https://www.yalemedicine.org/conditions/endometrial-hyperplasia

8. Mayo Clinic Staff. Endometriosis. Mayo Clinic. Published July 24, 2018. https://www.mayoclinic.org/diseases-conditions/endometriosis/symptoms-causes/syc-20354656
9. Medina-Perucha L, Pistillo A, Raventós B, et al. Endometriosis prevalence and incidence trends in a large population-based study in Catalonia (Spain) from 2009 to 2018. *Womens Health (Lond)*. 2022;18:17455057221130566. doi:10.1177/17455057221130566
10. Burney RO, Giudice LC. Pathogenesis and pathophysiology of endometriosis. *Fertil Steril*. 2012;98(3):511-519. doi:10.1016/j.fertnstert.2012.06.029
11. Parasar P, Ozcan P, Terry KL. Endometriosis: Epidemiology, Diagnosis and Clinical Management. *Current Obstetrics and Gynecology Reports*. 2017;6(1):34-41. doi:10.1007/s13669-017-0187-1
12. Lee SY, Koo YJ. Classification of endometriosis. *Yeungnam University Journal of Medicine*. 2021;38(1):10-18. doi:10.12701/yujm.2020.00444
13. Targarona EM, Balagué C, Knook MM, Trías M. Laparoscopic surgery and surgical infection. *Br J Surg*. 2000;87(5):536-544. doi:10.1046/j.1365-2168.2000.01429.x
14. Peterson CM, Johnstone E, Hammoud AO, et al. Risk factors associated with endometriosis: importance of study population for characterizing disease in the ENDO Study. *American Journal of Obstetrics and Gynecology*. 2013;208(6):451.e1-451.e11. doi:10.1016/j.ajog.2013.02.040
15. Tanha M, Bozorgmehr M, Shokri MR, et al. 2, 3, 7, 8-Tetrachlorodibenzo-p-dioxin potential impacts on peripheral blood mononuclear cells of endometriosis women. *Journal of Reproductive Immunology*. 2022;149:103439. doi:10.1016/j.jri.2021.103439

16. Yoshida I, Ishida K, Yoshikawa H, et al. In vivo profiling of 2,3,7,8-tetrachlorodibenzo-p-dioxin–induced estrogenic/anti-estrogenic effects in female estrogen-responsive reporter transgenic mice. *Journal of Hazardous Materials*. 2020;385:121526. doi:10.1016/j.jhazmat.2019.121526
17. John Hopkins Medicine. Endometriosis. John Hopkins Medicine. https://www.hopkinsmedicine.org/health/conditions-and-diseases/endometriosis
18. Endometriosis. *Yale Medicine*. August 2022. https://www.yalemedicine.org/conditions/endometriosis.
19. Nawrocka-Rutkowska J, Szydłowska I, Rył A, Ciećwież S, Ptak M, Starczewski A. Evaluation of the Diagnostic Accuracy of the Interview and Physical Examination in the Diagnosis of Endometriosis as the Cause of Chronic Pelvic Pain. *International Journal of Environmental Research and Public Health*. 2021;18(12):6606. doi:10.3390/ijerph18126606
20. Nezhat CH, Santolaya J, Nezhat F, Nezhat C. Comparison of transvaginal sonography and bimanual pelvic examination in patients with laparoscopically confirmed endometriosis. *Journal of the American Association of Gynecologic Laparoscopists*. 1994;1(2):127-130. doi:10.1016/s1074-3804(05)80775-3
21. Hsu AL, Khachikyan I, Stratton P. Invasive and Noninvasive Methods for the Diagnosis of Endometriosis. *Clinical Obstetrics and Gynecology*. 2010;53(2):413-419. doi:10.1097/grf.0b013e3181db7ce8
22. Ballantyne GH. The pitfalls of laparoscopic surgery: challenges for robotics and telerobotic surgery. *Surg Laparosc Endosc Percutan Tech*. 2002;12(1):1-5. doi:10.1097/00129689-200202000-00001

23. Gratton SM, Choudhry AJ, Vilos GA, et al. Diagnosis of Endometriosis at Laparoscopy: A Validation Study Comparing Surgeon Visualization with Histologic Findings. *Journal of Obstetrics and Gynaecology Canada*. 2022;44(2):135-141. doi:10.1016/j.jogc.2021.08.013
24. Wykes C, Clark TJ, Khan KM. REVIEW: Accuracy of laparoscopy in the diagnosis of endometriosis: a systematic quantitative review. *Blog: An International Journal of Obstetrics and Gynaecology*. 2004;111(11):1204-1212. doi:10.1111/j.1471-0528.2004.00433.x
25. Mettler L, Schollmeyer T, Lehmann-Willenbrock E, et al. Accuracy of laparoscopic diagnosis of endometriosis. *JSLS*. 2003;7(1):15-18.
26. El Bishry G, Tselos V, Pathi A. Correlation between laparoscopic and histological diagnosis in patients with endometriosis. *Journal of Obstetrics and Gynaecology*. 2008;28(5):511-515. doi:10.1080/01443610802217918
27. Worley MJ, Slomovitz BM, Ramirez PT. Complications of laparoscopy in benign and oncologic gynecological surgery. *Rev Obstet Gynecol*. 2009;2(3):169-175.
28. Zachariah R, Schmid S, Radpour R, et al. Circulating cell-free DNA as a potential biomarker for minimal and mild endometriosis. *Reproductive Biomedicine Online*. 2009;18(3):407-411. doi:10.1016/S1472-6483(10)60100-9
29. Florio P, Reis FM, Torres PB, et al. Plasma Urocortin Levels in the Diagnosis of Ovarian Endometriosis. *Obstetrics & Gynecology*. 2007; 110 (3): 594-600. doi: 10.1097/01.AOG.0000278572.86019.ae.

30. Anastasiu CV, Moga MA, Elena Neculau A, et al. Biomarkers for the Noninvasive Diagnosis of Endometriosis: State of the Art and Future Perspectives. *Int J Mol Sci*. 2020;21(5):1750. Published 2020 Mar 4. doi:10.3390/ijms21051750

31. Mol BWJ, Bayram N, Lijmer JG, et al. The performance of CA-125 measurement in the detection of endometriosis: a meta-analysis. *Fertility and Sterility*. 1998;70(6):1101-1108. doi:10.1016/s0015-0282(98)00355-0

32. Cheng Y. Serum CA-125 in preoperative patients at high risk for endometriosis. *Obstetrics & Gynecology*. 2002;99(3):375-380. doi:10.1016/s0029-7844(01)01731-8

33. Mihalyi A, Gevaert O, Kyama CM, et al. Non-invasive diagnosis of endometriosis based on a combined analysis of six plasma biomarkers. *Human Reproduction*. 2009;25(3):654-664. doi:10.1093/humrep/dep425

34. Xavier P, Beires J, Belo L, et al. Are we employing the most effective CA 125 and CA 19-9 cut-off values to detect endometriosis? *European Journal of Obstetrics & Gynecology and Reproductive Biology*. 2005;123(2):254-255. doi:10.1016/j.ejogrb.2005.04.003

35. Cho S, Cho H, Nam AS, et al. Neutrophil-to-lymphocyte ratio as an adjunct to CA-125 for the diagnosis of endometriosis. *Fertility and Sterility*. 2008;90(6):2073-2079. doi:10.1016/j.fertnstert.2008.03.061

36. Hoofnagle AN, Wener MH. The fundamental flaws of immunoassays and potential solutions using tandem mass spectrometry. *J Immunol Methods*. 2009;347(1-2):3-11. doi:10.1016/j.jim.2009.06.003

37. Wölfler M, Schwamborn K, Otten D, Hornung D, Liu H, Rath W. Mass spectrometry and serum pattern profiling for analyzing the individual risk for endometriosis: promising

insights? *Fertility and Sterility*. 2009;91(6):2331-2337. doi:10.1016/j.fertnstert.2008.03.064

38. Zheng N, Pan CT, Liu W. New Serum Biomarkers for Detection of Endometriosis Using Matrix-Assisted Laser Desorption/Ionization Time-of-Flight Mass Spectrometry. *Journal of International Medical Research*. 2011;39(4):1184-1192. doi:10.1177/147323001103900406
39. Dutta M, Singh BK, Joshi M, et al. Metabolomics reveals perturbations in endometrium and serum of minimal and mild endometriosis. *Scientific Reports*. 2018;8(1). doi:10.1038/s41598-018-23954-7
40. Zachariah R, Schmid S, Radpour R, et al. Circulating cell-free DNA as a potential biomarker for minimal and mild endometriosis. *Reproductive BioMedicine Online*. 2009;18(3):407-411. doi:10.1016/s1472-6483(10)60100-9
41. Ametzazurra A, Matorras R, Garcia-Velasco JA, et al. Endometrial fluid is a specific and non-invasive biological sample for protein biomarker identification in endometriosis. *Human Reproduction*. 2008;24(4):954-965. doi:10.1093/humrep/den450
42. Encalada Soto D, Rassier S, Green IC, Burnett T, Khan Z, Cope A. Endometriosis biomarkers of the disease: an update. *Current Opinion in Obstetrics & Gynecology*. 2022;34(4):210-219. doi:10.1097/GCO.0000000000000798
43. Professional CCM. Fluoroscopy. *Cleveland Clinic*. https://my.clevelandclinic.org/health/diagnostics/21992-fluoroscopy.
44. Kavoussi SK, Lim CS, Skinner B, Lebovic DI, As-Sanie S. New paradigms in the diagnosis and management of endometriosis. *Current Opinion in Obstetrics & Gynecology*. 2016;28(4):267-276. doi:10.1097/gco.0000000000000288

45. Intuitive Surgical Operations. Da Vinci Vision. *Intuitive*. Published June 2022. https://www.intuitive.com/en-gb/products-and-services/da-vinci/vision.

46. Notarstefano V, Gioacchini G, Byrne HJ, et al. Vibrational characterization of granulosa cells from patients affected by unilateral ovarian endometriosis: New insights from infrared and Raman microspectroscopy. *Spectrochimica Acta Part A: Molecular and Biomolecular Spectroscopy*. 2019;212:206-214. doi:10.1016/j.saa.2018.12.054

47. Bumbrah GS, Sharma R. Raman spectroscopy – Basic principle, instrumentation and selected applications for the characterization of drugs of abuse. *Egyptian Journal of Forensic Sciences*. 2016;6(3):209-215. doi:10.1016/j.ejfs.2015.06.001

48. Saletnik A, Saletnik B, Puchalski C. Overview of Popular Techniques of Raman Spectroscopy and Their Potential in the Study of Plant Tissues. *Molecules*. 2021;26(6):1537. doi:10.3390/molecules26061537

49. Li Lin, Xinyuan Bi, Yuqing Gu, Fu Wang, Jian Ye; Surface-enhanced Raman scattering nanotags for bioimaging. *Journal of Applied Physics*. 2021; 129 (19): 191101. doi:10.1063/5.0047578

50. Gautam R, Vanga S, Ariese F, Umapathy S. Review of multidimensional data processing approaches for Raman and infrared spectroscopy. *EPJ Techniques and Instrumentation*. 2015;2(1). doi:10.1140/epjti/s40485-015-0018-6

51. Jones RL, Hooper DC, Zhang L, Wolverson D, Valev VK. Raman Techniques: Fundamentals and Frontiers. *Nanoscale Research Letters*. 2019;14(1). doi:10.1186/s11671-019-3039-2

52. Koya AN, Zhu X, Ohannesian N, et al. Nanoporous Metals: From Plasmonic Properties to Applications in Enhanced Spectroscopy and Photocatalysis. *ACS Nano*. 2021;15(4):6038-6060. doi:10.1021/acsnano.0c10945

53. Kong K, Kendall C, Stone N, Notingher I. Raman spectroscopy for medical diagnostics — From in-vitro biofluid assays to in-vivo cancer detection. *Advanced Drug Delivery Reviews*. 2015;89:121-134. doi:10.1016/j.addr.2015.03.009

54. Huang Z, McWilliams A, Lui H, McLean DI, Lam S, Zeng H. Near-infrared Raman spectroscopy for optical diagnosis of lung cancer. *International Journal of Cancer*. 2003;107(6):1047-1052. doi:10.1002/ijc.11500

55. Magee ND, Beattie JK, Carland C, et al. Raman microscopy in the diagnosis and prognosis of surgically resected nonsmall cell lung cancer. *Journal of Biomedical Optics*. 2010;15(2):026015. doi:10.1117/1.3323088

56. Parlatan U, Inanc MT, Ozgor BY, et al. Raman spectroscopy as a non-invasive diagnostic technique for endometriosis. *Scientific Reports*. 2019;9(1):19795-19797. doi:10.1038/s41598-019-56308-y

57. Guleken Z, Bulut H, Bulut B, Paja W, Parlinska-Wojtan M, Depciuch J. Correlation between endometriomas volume and Raman spectra. Attempting to use Raman spectroscopy in the diagnosis of endometrioma. *Spectrochimica acta Part A, Molecular and biomolecular spectroscopy*. 2022;274:121119-. doi:10.1016/j.saa.2022.121119

58. Nayyar T, Bruner-Tran KL, Piestrzeniewicz-Ulanska D, Osteen KG. Developmental exposure of mice to TCDD elicits a similar uterine phenotype in adult animals as observed in women with endometriosis. *Reprod Toxicol*. 2007;23(3):326-336. doi:10.1016/j.reprotox.2006.09.007

59. Vercellini P, Viganò P, Bandini V, Buggio L, Berlanda N, Somigliana E. Association of endometriosis and adenomyosis with pregnancy and infertility. *Fertil Steril*. 2023;119(5):727-740. doi:10.1016/j.fertnstert.2023.03.018

60. Rier S, Foster WG. Environmental dioxins and endometriosis. *Semin Reprod Med*. 2003;21(2):145-154. doi:10.1055/s-2003-41321

61. Foster WG. Endocrine toxicants including 2,3,7,8-terachlorodibenzo-p-dioxin (TCDD) and dioxin-like chemicals and endometriosis: is there a link?. *J Toxicol Environ Health B Crit Rev*. 2008;11(3-4):177-187. doi:10.1080/10937400701873456

62. Stephens VR, Rumph JT, Ameli S, Bruner-Tran KL, Osteen KG. The Potential Relationship Between Environmental Endocrine Disruptor Exposure and the Development of Endometriosis and Adenomyosis. *Front Physiol*. 2022;12:807685. Published 2022 Jan 28. doi:10.3389/fphys.2021.807685

# *CHAPTER II: IN VITRO INVESTIGATION OF ENDOMETRIOSIS MODELS VIA RAMAN-BASED MEASUREMENTS*

## Specific Aims

Endometriosis is a common and often debilitating gynecologic condition that has impacted the health of millions of reproductive-age women. Patients afflicted with endometriosis generally are not accurately diagnosed until 8-10 years after the onset of the disease.[1] Such delayed diagnoses result in disease progression and the development of more severe symptoms, such as exceptional pain, intrauterine adhesions, and infertility. Currently, the only reliable method for accurate endometriosis diagnosis is a laparoscopy – an invasive procedure that requires skilled surgeons and proper medical equipment.[2] Therefore, there is a significant need to develop a minimally invasive technique to accurately detect early-stage endometriosis to prevent disease progression and yield better patient outcomes. In this study, we utilized both human and murine *in vitro* models to garner insight into the biochemical signatures of cellular secretions derived from tissues exhibiting the endometriosis phenotype. Our central hypothesis was that Raman-based measurements – traditional Stokes Raman spectroscopy coupled with the surface plasmon resonance (SPR) effect – augment Raman signal and enable the identification of important biomolecules during the development of endometriosis to be later confirmed via mass spectroscopy. Herein, using human endometrial stromal cells in addition to murine bone marrow derived macrophages, we explored the viability of Raman-based measurements in distinguishing between healthy and inflamed cells and those displaying the endometriosis phenotype as induced by the environmental toxicant, 2,3,7,8-tetrachlorodibenzo-*p*-dioxin (TCDD).

**<u>Specific Aim 1</u>: Evaluate the effectiveness of Raman-based measurements to differentiate the responses of murine bone marrow-derived macrophages following exposure to environmental toxicants.** In this aim, we sought to determine the effect of toxic exposure on murine bone marrow-derived macrophages. Using Raman-based measurements, we endeavored to distinguish between the composition of the cellular secretions of samples representing healthy, inflamed, and endometriotic cells. To circumvent the low scattering efficiency of RS for biological specimens, we utilized the SPR effect via an aluminum substrate.

**<u>Specific Aim 2</u>: Evaluate the effectiveness of Raman-based measurements to differentiate the responses of human cells endometrial stromal cells following exposure to environmental toxicants.** In this aim, we sought to determine the effect of toxic exposure on human endometrial stromal cells. Using Raman-based measurements, we endeavored to distinguish between the composition of the cellular secretions of samples representing healthy, inflamed, and endometriotic cells. An aluminum substrate was used to attain augmented Raman signal via the SPR effect.

The results of these aims provide insight into the toxicant-mediated response and biochemical signature of endometriosis. Given the current dearth of definitive biomarkers, such findings could improve diagnostic capabilities, enable prompter and more effective treatment, and limit disease progression. Furthermore, employing the synergistic principles of the surface plasmon resonance (SPR) effect and droplet vaporization patterns enables augmented Raman signal intensity with high repeatability. The refinement of such an approach has the potential to result in the future development of a label-free diagnostic tool that reliably detects early-stage endometriosis – a disease increasing in prevalence worldwide – in reproductive-age women.

## Introduction

Across the past few decades, several technological advancements have revolutionized the landscape of biomedical research. This paper has already discussed the adaptation of Raman spectroscopy for disease diagnostic purposes.[3] Another class of the innumerable scientific developments that has become more refined in recent years is the lab-on-a-chip (LOC). Lab-on-a-chip models are scaled-down devices capable of integrating numerous processes and analyses into a single controlled, consolidated environment. These models have demonstrated exceptional utility in a variety of fields, including pharmacology, analytical chemistry, and molecular biology.[4] Within the pathological context, the emergence of LOC models has enabled unprecedented rates of medical discovery. The ability to accurately and rapidly simulate physiologic conditions is providing invaluable insight into disease progression, resulting in the development of novel diagnostic and therapeutic strategies.[4] LOC models have the potential to continue transforming biomedical research efforts, accelerating disease diagnosis and treatment, and ultimately, improving patient outcomes.

LOC models have made substantial contributions towards understanding the pathophysiology of several diseases. Once understood, scientists can manipulate LOCs to represent pathological progression with more accuracy in order to effectively determine disease hallmarks and evaluate drug efficacy. Furthermore, LOC models enable improved experimentation speeds at lower costs and resource consumption. These platforms have been used to efficiently determine cell proliferation rates for hepatocellular carcinoma, assess cardiomyocyte function in response to anti-fibrotic drugs, emulate the first pass metabolic effect of the gastrointestinal tract, screen therapeutics for renal disease.[5,6,7,8] In many of these cases, LOCs drastically reduced capital costs, augmented throughput, provided better simulated

physiological conditions, and improved overall knowledge pertaining to disease signatures (i.e. biomarkers). Furthermore, the impact of LOC models is not exclusive to research settings. LOCs are currently being used for a plethora of population-level diseases.[9,10] Their excellent throughput, cost-effectiveness, and portability render them highly useful within diagnostic contexts. Examples of accurate and efficient diagnoses of viral diseases, such as Ebola, AIDS, measles, and SARS-CoV-2, and chronic diseases (i.e., diabetes, respiratory conditions, sickle cell anemia, etc.) have demonstrated the clinical translatability of LOC models as well as their potential to create a profound impact on global health.[9,10]

One particular group has focused on developing LOCs for endometrial modeling. In the past, the complex hormone-dependent environment of the endometrium has been difficult to accurately simulate. Biological functions and conditions such as cell-cell communication, hemodynamic-induced forces (i.e., shear stress), and cytoskeleton remodeling have been physiologically inaccurate in previous *in vitro* models. In order to address this issue and establish a more comprehensive and accurate modeling system, the Osteen lab has created microfluidic devices to enable physiologically relevant monitoring of controlled endometrial environments. The 3D microfluidic cell culture devices, coined organs-on-a-chip (OoC), contain multiple cell chambers, are transparent, on the microscale, and made from a porous and non-cytotoxic resin. This design permits rapid diffusion, cell-cell communication, fluorescence imaging, relevant shear stress, as well as a viable environment for the long-term co-culturing of different cell types. Such OoCs have been utilized to study human endometrial stromal cells, endothelial cells, amnion epithelial cells, and decidual cells among others in order to effectively analyze endometrium cells under various conditions. Endometrium OoC models are powerful *in vitro*

tools with the potential to provide accurate insight into the progression of a myriad of physiologic and pathophysiologic processes within the reproductive tract. [11,12]

LOC technology is still quite novel and constantly improving; however, innumerable studies have already proven its extensive and effective utility for biomedical discovery. Herein, we seek to establish an effective baseline methodology (without potential confoundment by LOC models) using standard cell culture techniques in order to differentiate between the cellular secretions of healthy, inflamed, and endometriotic cells using Raman-based measurements. In subsequent studies, we will employ the LOC approach to more accurately model the disease progression of TCDD-induced endometriosis in order to garner insight into its underlying biochemical signature.

## Methods

### *Sample Collection*

The *in vitro* samples, both murine and human, were obtained in collaboration with the Bruner-Tran and Osteen labs at Vanderbilt University Medical Center using standard cell culture techniques. Including the control media, there were a total of nine samples among two different cell types and four exposure groups (Table 3; Figure 7).

**Table 3.** Experimental sample dataset.

| Sample Name | Origin | Exposure Type |
|---|---|---|
| 1A | Human Endometrial Stromal Cells | Control (CT) |
| 2A | Human Endometrial Stromal Cells | LPS |
| 3A | Human Endometrial Stromal Cells | TCDD |
| 4A | Human Endometrial Stromal Cells | LPS + TCDD |
| 5A | Murine Bone Marrow Derived Macrophages | Control |
| 6A | Murine Bone Marrow Derived Macrophages | LPS |
| 7A | Murine Bone Marrow Derived Macrophages | TCDD |
| 8A | Murine Bone Marrow Derived Macrophages | LPS + TCDD |
| EM | Experimental Media | N/A |

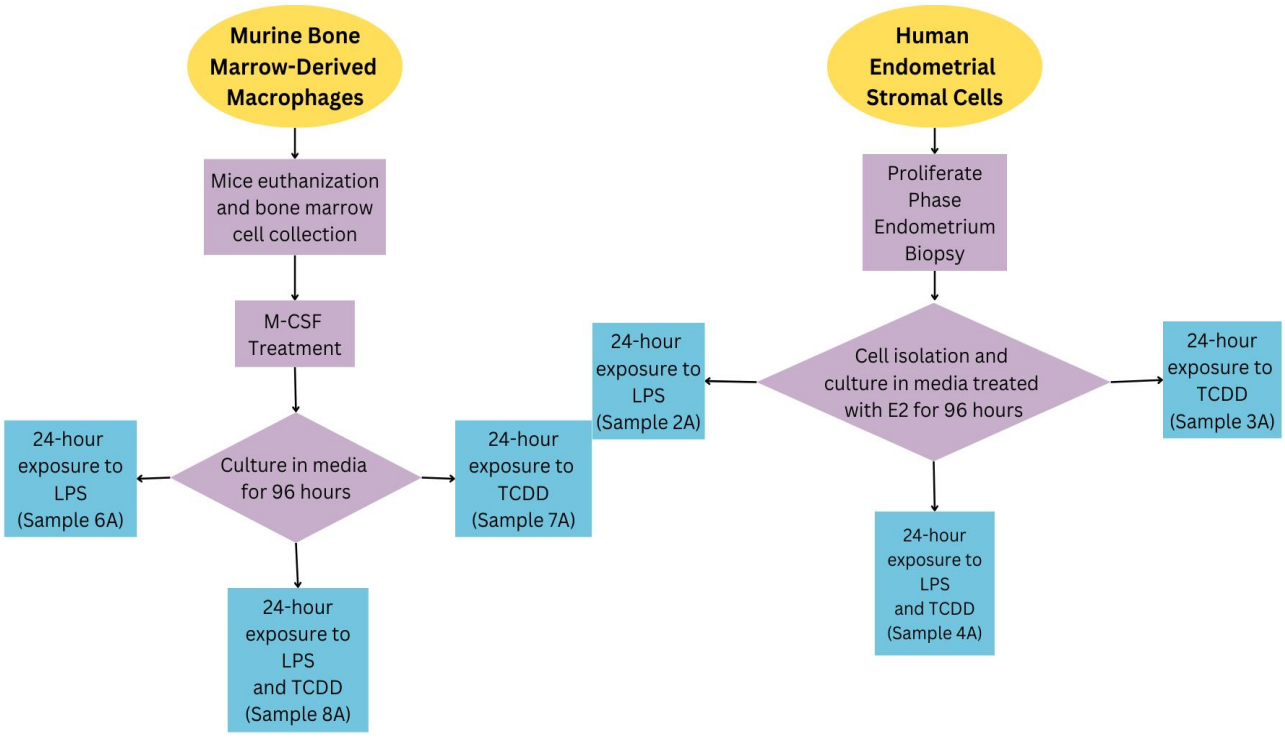


**Figure 7.** Cell collection and treatment process. Control samples not pictured. Murine bone marrow-derived macrophages (left); human endometrial stromal cells (right).

**Murine Samples.** Mice were bred and raised under the provision of the Division of Animal Care at Vanderbilt University Medical Center. In this study, one murine cell type was utilized: bone marrow-derived macrophages. Macrophages were observed in order to evaluate the innate immune response following TCDD and/or LPS exposure. The cellular secretions within the reproductive tract differ significantly between immune cells and endometrial cells.

For the bone marrow-derived macrophages, mice were euthanized during estrus, a period in the female mammal reproductive cycle characterized by high sexual proceptivity and receptivity, and bone marrow cells were collected from their femurs and tibias. The extracted cells were then treated with macrophage colony-stimulating factor (M-CSF) in order to induce differentiation into macrophages. Afterwards, the resulting macrophages were cultured in the experimental control media for 96 hours. Depending on the treatment group, this was followed

by 24-hour exposure to LPS- and/or TCDD-treated media. The conditioned media of each group was collected. Once the final samples were collected, they were frozen and stored at -80°C.

**Human Samples.** Human endometrial stromal cells were derived from a single non-endometriosis patient at the Vanderbilt University Medical Center clinic. Following a proliferative phase endometrium biopsy, cells were isolated via a series of enzymatic digestion reactions and filtrations.[20] The isolated endometrial stromal cells were then cultured in the control media with estradiol (E2) for 96 hours. Afterwards, these cells were separated into their respective treatment groups where LPS and/or TCDD were added to the media for 24 hours. The conditioned media of each group were collected. Once the final samples were collected, they were frozen and stored at -80°C.

***Drop-Cast Raman Measurement Protocol***

25x75x1mm glass slides were wrapped in aluminum foil with minimal creases. The aluminum foil was securely attached to the glass slides with tape, splitting the slide into three distinct sections that were labeled with the appropriate sample number. Samples were then retrieved from the -80°C freezer and set aside in a test tube rack to thaw at room temperature for 30 minutes. Once the time had elapsed, the samples were inverted three times to ensure a fully melted and homogenous redistribution of solutes within the media. Next, three 5μL droplets of each sample were pipetted onto an aluminum foil-wrapped slide within its respective section (Fig. 8). To mitigate the risk of sample contamination, pipette tips were replaced after each droplet. Upon the completion of the triplicate droplets of one sample, a 30-minute dry period was allotted prior to collecting measurements.

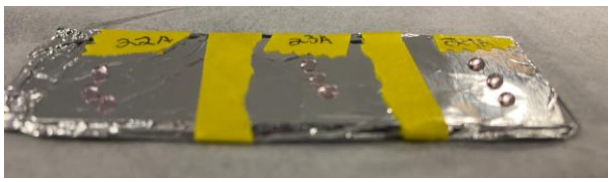

**Figure 8.** Triplicate droplet technique.

A Renishaw inVia$^{TM}$ confocal Raman microscope (West Dundee, IL) was utilized for Raman spectroscopic measurements. Prior to data collection, the instrument was calibrated to ensure a sufficient laser count and accurate Raman shift under 785nm excitation (i.e., 30,000+ counts and ~520.4 $cm^{-1}$ peak, respectively) for the system's internalized silica standard. Following successful calibration, a 2-second integration time with 10 accumulations was performed at ten distinct locations (five edge measurements, five center measurements) within each dried droplet with a power between 52 and 55mW under a 20x magnification objective lens. This process was repeated for each of the three dried droplets for a total of n = 30 measurements per each sample. Furthermore, the experimental media was also measured using the same process. In the event of apparent fluorescence saturation or inexplicable spectral spikes, the same measurement was repeated. Additionally, samples were checked for thermal damage after each measurement. Another key element to note is that spectroscopic readings were performed in the fingerprint region (i.e., 600-1750$cm^{-1}$).

Following each session, measurements were performed in order to determine which spectral regions could be solely attributed to Raman signal from the sample of interest and which were due to the background substrate (i.e., aluminum foil-wrapped glass slide). Using the same Raman parameters (i.e., 2-second integration time, 10 accumulations, 52-55mW laser power, 785nm laser, and 20x lens), measurements were collected from five different areas where dried droplets were not present.

Upon the completion of the data collection, each Raman spectrum was saved and exported as a .txt file for data processing and analysis.

***Raman Data Processing***

Raman spectral files were uploaded to and processed in MATLAB. First, a 2nd order Savitzky-Golay filter (window size = 7) was applied to smooth each spectrum. Then, spectral background fluorescence was subtracted based on a 7th order polynomial fit technique developed by the Mahadevan-Jansen Lab in 2003.[13]The resulting spectra were mean normalized and imported into OriginLab for data analysis (Fig. 9). These progressive processes serve to improve the signal-to-noise ratio and enable comparisons between Raman spectra.

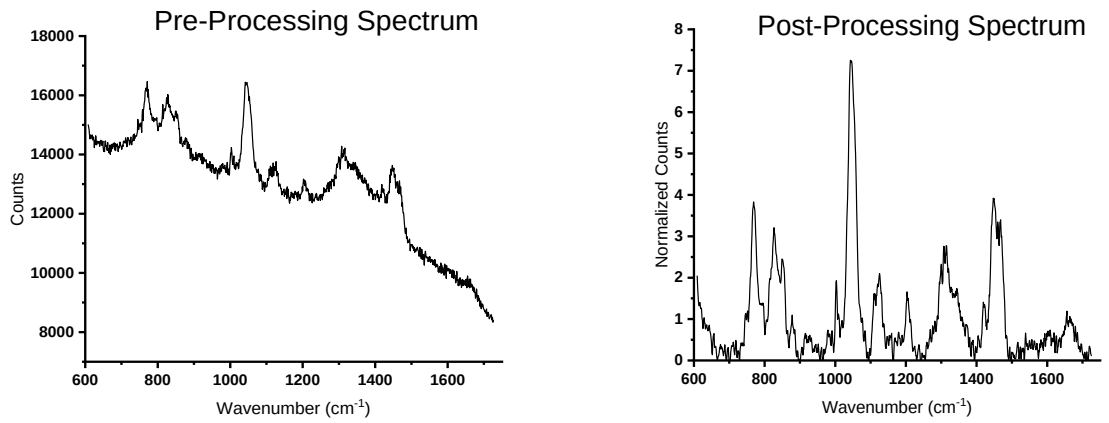


**Figure 9.** Raman spectral processing. Pre-processed spectrum (left); post-processed spectrum (right).

***Raman Spectral Analysis***

The exported Raman spectra were separated into two measurement types: edge and center of the dried droplet. The triplicate droplet method and five measurements performed per droplet result in 135 spectra across the nine samples for each region (i.e., edge and center; 270 total spectra). Using OriginLab, the five post-processed spectra from each droplet were averaged and plotted on y-offset graphs along with the averaged background aluminum foil Raman spectrum. All plots were sufficiently labeled.

Once plotted, peaks were then identified and correlated to biomolecules based on established findings in literature.[14] The spectral peaks generally corresponded with various proteins, nucleic acids, lipids, and other macromolecules (Fig. 10). Additionally, peak intensity differences between edge and center measurements were visually examined and reported.

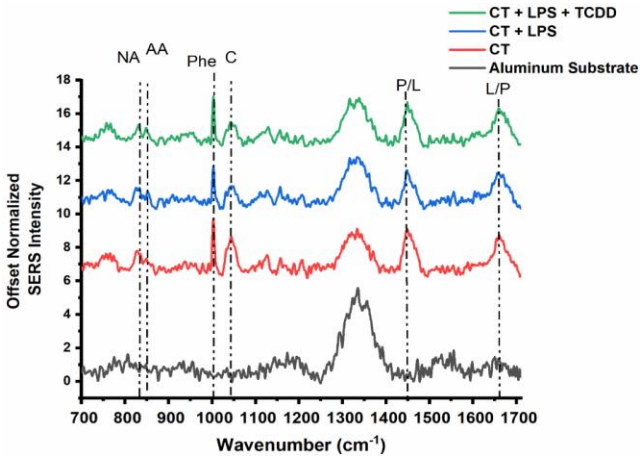


**Figure 10.** Example of averaged Raman spectra. NA = nucleic acid; AA = amino acids; Phe = phenylalanine; C = carbohydrates; P/L = proteins/lipids; L/P = lipoproteins.

Furthermore, in order to determine the variation between samples, principal component analysis (PCA) was performed between each treatment group for each cell type (i.e., human endometrial stromal cells and trophoblasts; murine bone marrow-derived macrophages). PCA is a statistical analysis technique used for dimensionality reduction and comparison of complex datasets. In the case of Raman spectra, wavenumbers are simplified to principal components which preserve the direction and magnitude of variances of the original data in the form of eigenvectors and eigenvalues. This enables the direct comparison of two sets of normalized Raman spectra across all wavenumbers simultaneously, allowing for a statistical distinguishment among peak intensities. The PCA plots were calculated and obtained from OriginLab. Only principal components with magnitudes greater than 0.05 were considered as significant peaks of variation. Additionally, principal components within the region of the background aluminum signal were disregarded.

## Results

### *Optimizing Raman Spectroscopy Measurement Parameters*

Initially, there were issues with determining the appropriate parameters and conditions for obtaining ideal Raman spectroscopy measurements. Early experiments varied in sample volume, laser power, and substrate material. After insufficient Raman signal using microplate wells, the substrate for Raman readings transitioned to glass slides, and eventually aluminum foil-wrapped glass slides. With each substitution, spectral intensity progressively improved. As a result of the SPR-enhanced signal, sample droplet volume was able to be decreased from 10μL to 5μL without compromising Raman efficiency. Additionally, the laser power was also decreased from 105-112mW to 52-55mW. From these preliminary experiments, we concluded that the optimal parameters for Raman-based analysis of the human and murine samples were a dried 5μL droplet on an aluminum foil-wrapped glass slide, laser power between 52mW and 55mW, 10 accumulations, and 2-second exposure time.

### *Spectral Peak Detection*

Following post-processing and spectral averaging (n = 5) per droplet, the Raman spectra for each sample (3 edge; 3 center) was plotted on the same graph (y-offset) along with the background aluminum foil spectrum. The graphs consistently displayed peak regions at 750-788, 810-830, 830-855, 1003-1004, 1043-1095, 1117-1123, 1210-1220, 1440-1449, and 1655-1680 $cm^{-1}$ across both the murine and human samples (Fig. 11-12; red plot titles indicate murine samples; black plot titles indicate human samples).

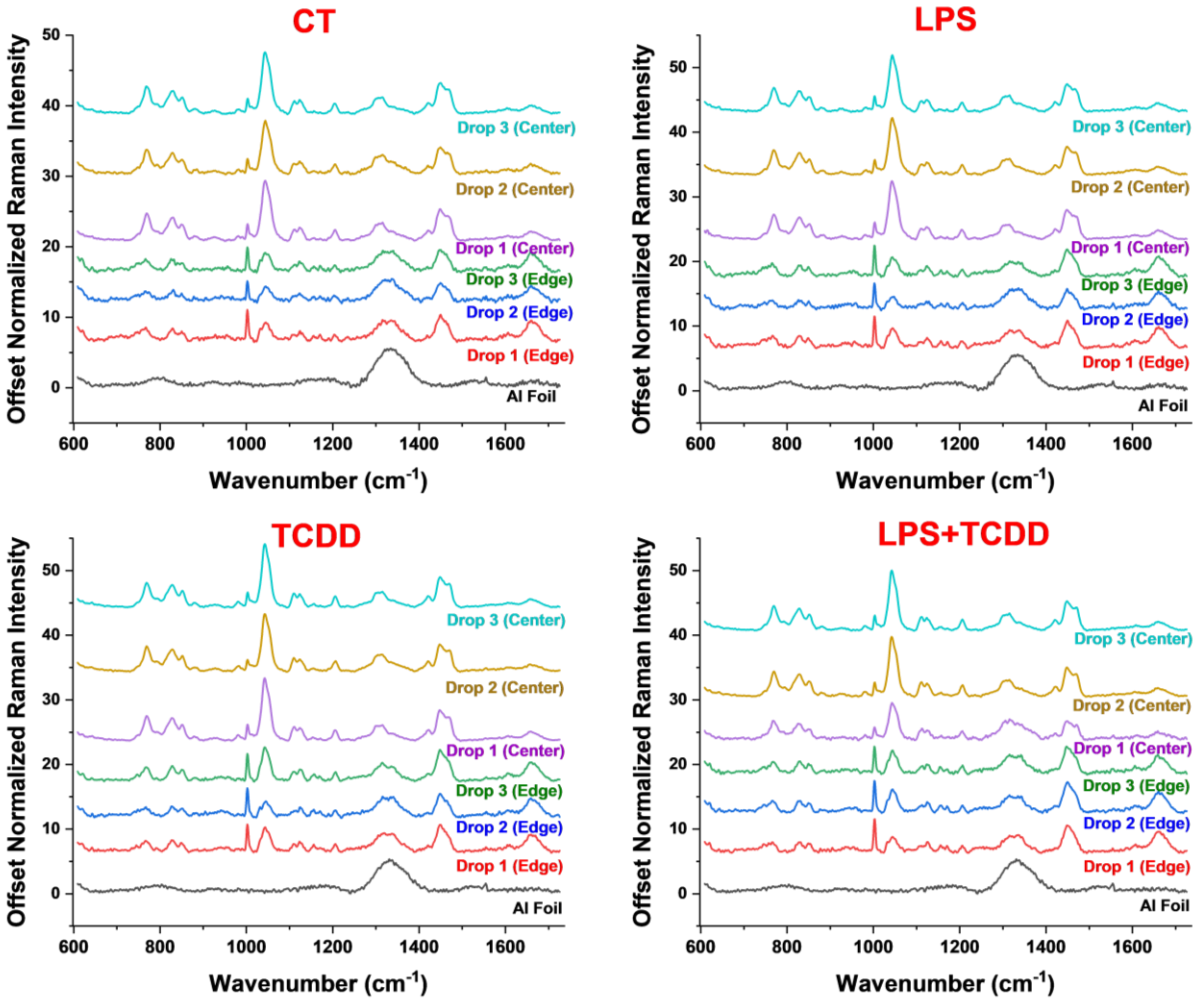


**Figure 11**. Raman spectra of murine bone marrow-derived macrophages.

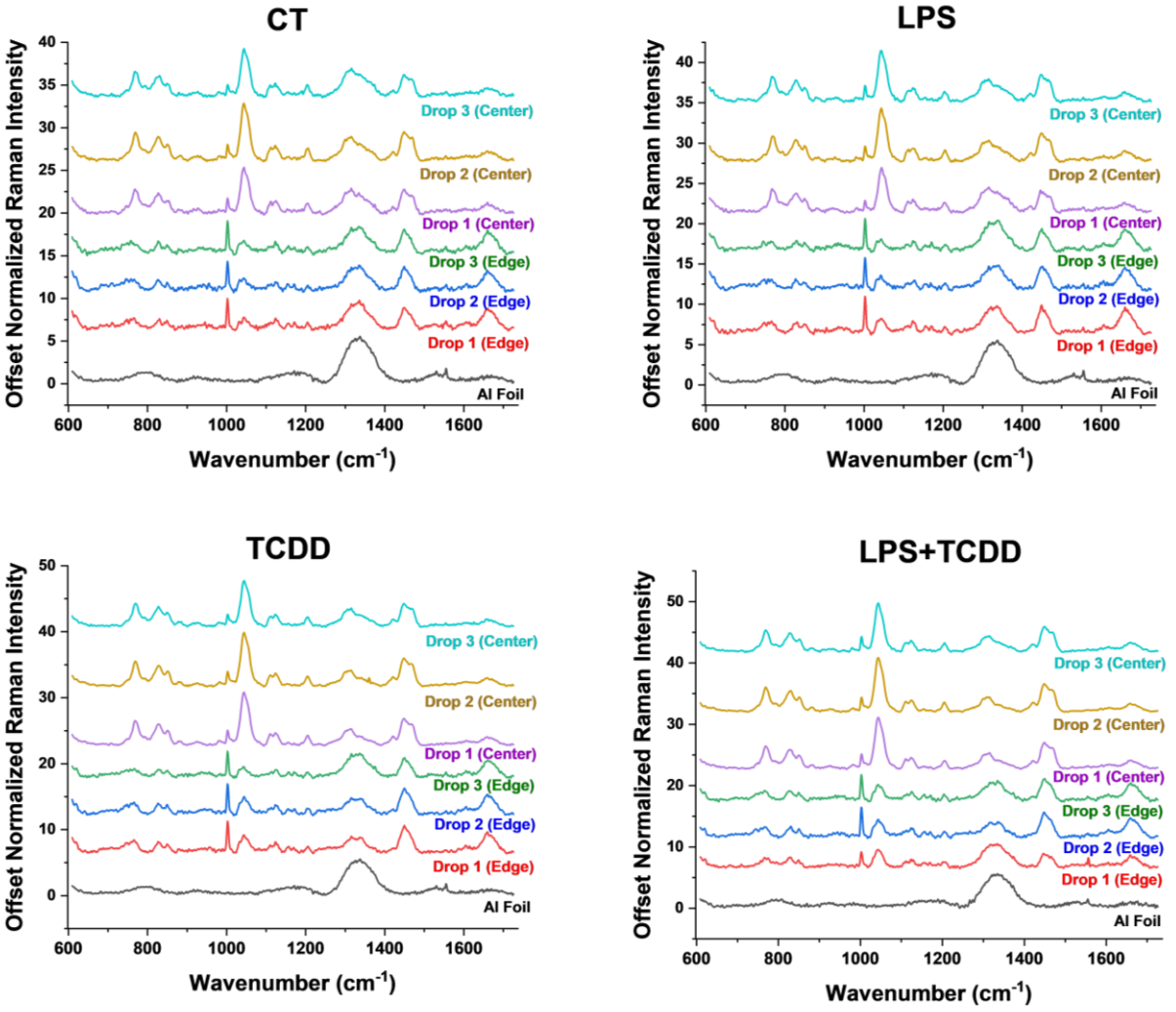


**Figure 12.** Raman spectra of human endometrial stromal cells.

The peaks correspond to tryptophan/nucleic acids (750-788cm$^{-1}$), nucleic acids (810-830cm$^{-1}$), amino acids (tyrosine, proline, and valine; 830-855cm$^{-1}$), phenylalanine (1003-1004cm$^{-1}$), carbohydrates (1043-1095cm$^{-1}$), glucose (1117-1123cm$^{-1}$), nucleic acids/amino acids (1200-1210cm$^{-1}$), proteins/lipids (1440-1449cm$^{-1}$), and lipoproteins (1655-1680cm$^{-1}$) (Table 4).[14] Furthermore, the aluminum foil substrate exhibited a background signal from 1250-1410cm$^{-1}$. As a result, any peaks from the samples within this region were disregarded.

**Table 4.** Raman peak correlation table.[14,15]

| Raman Shift ($cm^{-1}$) | Vibrational Source | Biochemical |
|---|---|---|
| 750-788 | Symmetric breathing; δ(ring) | Tryptophan/Nucleic Acids |
| 810-830 | O—P—O stretching | Nucleic Acids |
| 830-855 | ν(C—C ) | Amino Acids (i.e., Tyrosine, Proline, Valine) |
| 1003-1004 | $\nu_s$(C—C ) breathing | Phenylalanine |
| 1043-1095 | C—O, C—C stretching | Carbohydrates |
| 1117-1123 | COH bending | Glucose |
| 1200-1210 | Ring breathing modes; Amide III stretching | Nucleic Acids/Amino Acids |
| 1440-1449 | δ($CH_2$); methylene bending | Proteins/Lipids |
| 1655-1680 | Amide I ν(C=C ) | Lipoproteins |

Although peak locations between all samples appeared similar, there were noticeable trends in peak intensity. The edge measurements consistently showcased greater peak heights at 1003 and 1655-1680 $cm^{-1}$ along with diminished peak heights at 750-788, 810-830, 1043-1095, and 1117-1123 $cm^{-1}$. Upon inspection, it was found that the experimental media also consisted of peaks that closely aligned with the intensities displayed in the center measurements from the samples. This could possibly be attributed to biomolecules from the media being retained in the sample's center instead of diffusing toward the edge during drying. Therefore, moving forward, only edge measurements underwent further data processing and analysis.

***Raman Data Analysis***

**Principal Component Analysis.** After pre-processing and averaging (per droplet) in OriginLab, Principal Component Analysis (PCA) was conducted to determine the extent of variability amongst the Raman spectra. The PCA results across different treatment groups and between human and murine samples showed that the primary peaks of variation were 1003, 1043-1095, 1440-1449, and 1655-1680 $cm^{-1}$. Less frequent peaks of variation included 810-830 and 830-855 $cm^{-1}$.

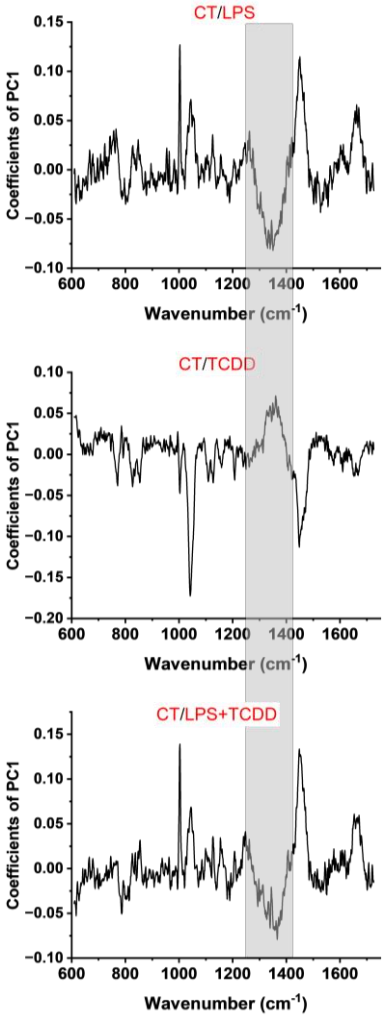


**Figure 13.** PCA plots for murine bone marrow-derived macrophages. Gray shaded box = aluminum region.

PCA plots of the murine bone marrow-derived macrophages indicated differences in Raman peak intensities following exposure to LPS and/or TCDD (Fig. 13). Relative to the control measurements (Sample 5A), the composition of the cellular secretions of the macrophages exposed to LPS (Sample 6A), TCDD (Sample 7A), and LPS + TCDD (Sample 8A) differed significantly. The LPS group exemplified high variance at the 1003, 1043-1095, 1440-1449, and 1655-1680 $cm^{-1}$ peaks. The TCDD group showed decreased intensities at the 1043-1095 and 1440-1449 $cm^{-1}$ peaks. The LPS + TCDD group exhibited similar Raman signal variances to the LPS group.

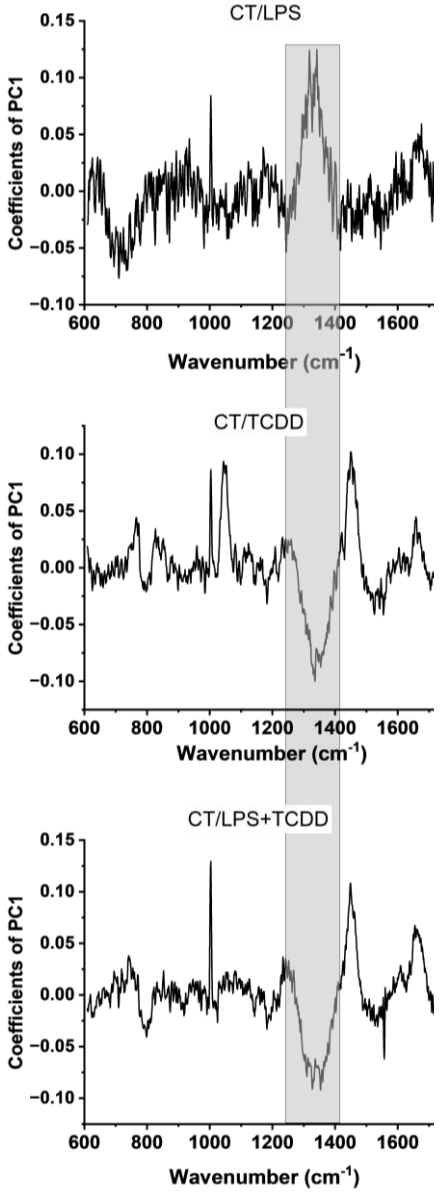


**Figure 14.** PCA plots for human endometrial stromal cells. Gray shaded box = aluminum region.

Similarly, the PCA plots of the human endometrial stromal cells indicated differences in Raman peak intensities following exposure to LPS and/or TCDD (Fig. 14). Relative to the control measurements (Sample 1A), the composition of the cellular secretions of the endometrial cells exposed to LPS (Sample 2A), TCDD (Sample 3A), and LPS + TCDD (Sample 4A) differed significantly. The LPS group exemplified variance at the 700-745, 1003, and 1655-1680 $cm^{-1}$. The TCDD group showed differences at the 810-830, 1003, 1043-1095, 1440-1449, and 1655-1680 $cm^{-1}$ peaks. The LPS + TCDD group exhibited differences at the 1003, 1440-1449, and 1655-1680 $cm^{-1}$ peaks.

PCA plots between the human endometrial stromal cells and the murine bone marrow-derived macrophages also displayed variances in Raman peak intensities across different animal cell types, despite similar treatment methods (Fig. 15). The murine control group demonstrated differences at the 750-788, 810-830, 1003, 1043-1095, and 1440-1449 $cm^{-1}$ peaks compared to the human control group. The LPS group exemplified variance at the 750-788, 1003, 1043-1095, and 1440-1449 $cm^{-1}$ peaks. The TCDD group showed differing signal intensities at the 750-788, 810-830, 1043-1095, and 1440-1449 $cm^{-1}$ peaks. The

LPS + TCDD group exhibited spectral differences at the 1003, 1440-1449, 1573-1579, and 1655-1680 $cm^{-1}$ peaks.

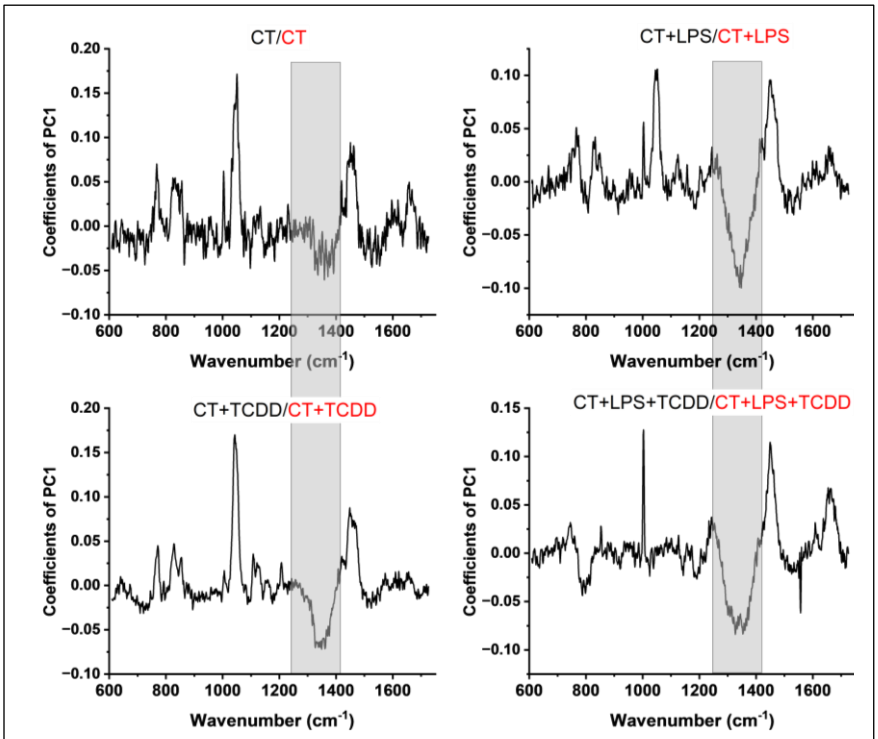


**Figure 15.** Inter-sample PCA plots between human endometrial stromal cells and murine bone marrow-derived macrophages. Gray shaded box = aluminum region.

**Discussion**

This study analyzed the cellular secretions of human and murine cells to assess the biochemical changes associated with TCDD exposure as a proof of concept for future studies examining cells from women with endometriosis. Raman spectroscopy was utilized to evaluate the different responses of tissue following exposures that induced the endometriosis phenotype.

First, the data processing methods were largely successful in improving SNR through the smoothing of data, removal of background fluorescence, and mean normalization of spectra. The post-processed data facilitated comparison between spectra and ensured that intensities could be solely attributed to Raman signal. Additionally, modifications to Raman analysis methods (i.e.,

transition from wet to dried droplets, increased accumulations, increased exposure times, and introduction of a plasmonic substrate) resulted in enhanced Raman scattering efficiency. Furthermore, minimal discrepancies between droplets of the same sample indicate the repeatability of this approach as mediated by the characteristic ring formation upon droplet evaporation. Moreover, the ability to consistently obtain Raman spectra with easily identifiable peaks facilitated subsequent analytical efforts.

The spectral peak locations remained consistent across samples. The 750-788, 810-830, 830-855, 1003, 1043-1095, 1440-1490, and 1655-1680 $cm^{-1}$ peak regions correspond to tryptophan/nucleic acids, nucleic acids, tyrosine, phenylalanine, carbohydrates, proteins/lipids, and lipoproteins, respectively.[14] Given the essential nature of these biomolecules within metabolic processes, their Raman presence was expected; however, the lack of evident peak location variability amongst the different treatment groups (control, LPS, and TCDD) was not expected. This could potentially be attributed to the short-lived exposure of the cells to the environmental toxicants. If toxic exposure exceeded 24 hours, it is possible that the molecular composition of the cellular secretions would have contained chemical modifications (i.e., phosphorylation, methylation, acetylation, etc.) resulting in slight differences in peak locations.

Although differences were not discernable on the basis of peak location, PCA results suggested variations in normalized peak intensities between samples. For the murine bone marrow-derived macrophages, differences in phenylalanine ($1003cm^{-1}$), carbohydrate ($1053cm^{-1}$), protein/lipid ($1455cm^{-1}$), and lipoprotein ($1655cm^{-1}$) content following LPS exposure were consistent with inflammatory responses in immune cells. LPS binds to CD14 receptors of macrophages to promote protein expression and cytokine secretion of tumor necrosis factor alpha (TNF-α), interleukin-1 (IL-1), interleukin-6 (IL-6), and interleukin-10 (IL-10), as the bone

marrow-derived macrophages mount an immune response.[16] The TCDD group exhibited differences in carbohydrate and protein/lipid content which could potentially be attributed to the toxicant's ability to effectively suppress immune function by limiting cytokine secretion.[17,18] Following these discoveries in murine models, we sought to determine whether such clear distinctions in biochemical composition translated to human cellular secretions. In the human endometrial stromal cells, variations in phenylalanine, lipoprotein, and tryptophan/nucleic acid (750-788$cm^{-1}$) content after LPS treatment suggest, similarly to the murine bone marrow-derived macrophages, that such exposure induces a proliferative response mediated by inflammatory cytokines.[19] The TCDD treatment group showcased increases in tryptophan/nucleic acids (750-788$cm^{-1}$), phenylalanine, carbohydrate, protein/lipid, and lipoprotein content which corroborate the aforementioned estrogenic effects of dioxin exposure (i.e. endometrial growth).[18] These findings suggest that the biochemical changes induced through toxic exposure (i.e. LPS and endometriosis-linked TCDD) were identifiable by Raman spectroscopy-based measurements in both murine bone marrow-derived macrophages and human endometrial stromal cells. Additionally, the results displayed distinct responses between acute inflammation (i.e., LPS) and endometriosis-like (i.e., TCDD) samples.

These results suggest that Raman spectroscopy has potential to be an effective analytical approach for differentiating between normal, inflammatory, and endometriotic responses via biochemical cellular secretions. Additionally, the expression patterns of macrophages and endometrial stromal cells following exposure to TCDD – an environmental toxicant which may promote endometriosis – provide insight into the biochemical signature of this disease. However, a larger sample size is needed to confirm these preliminary findings.

## References


1. Endometriosis. *Yale Medicine*. Published August 2022. https://www.yalemedicine.org/conditions/endometriosis.
2. Mayo Clinic Staff. Endometriosis. Mayo Clinic. Published July 24, 2018. https://www.mayoclinic.org/diseases-conditions/endometriosis/symptoms-causes/syc-20354656
3. Kong K, Kendall C, Stone N, Notingher I. Raman spectroscopy for medical diagnostics — From in-vitro biofluid assays to in-vivo cancer detection. *Advanced Drug Delivery Reviews*. 2015;89:121-134. doi:10.1016/j.addr.2015.03.009
4. Neuži P, Giselbrecht S, Länge K, Huang TJ, Manz A. Revisiting lab-on-a-chip technology for drug discovery. *Nat Rev Drug Discov*. 2012;11(8):620-632. doi:10.1038/nrd3799
5. Piccinno E, Monteduro AG, Dituri F, Rizzato S, Giannelli G, Maruccio G. Validation of a Lab-on-Chip Assay for Measuring Sorafenib Effectiveness on HCC Cell Proliferation. *International Journal of Molecular Sciences.* 2021;22(23):13090-. doi:10.3390/ijms222313090
6. Mastikhina O, Moon BU, Williams K, et al. Human cardiac fibrosis-on-a-chip model recapitulates disease hallmarks and can serve as a platform for drug testing. *Biomaterials*. 2020;233:119741-119741. doi:10.1016/j.biomaterials.2019.119741
7. Choe A, Ha SK, Choi I, Choi N, Sung JH. Microfluidic Gut-liver chip for reproducing the first pass metabolism. *Biomed Microdevices*. 2017;19(1):4. doi:10.1007/s10544-016-0143-2

8. Yin L, Du G, Zhang B, et al. Efficient Drug Screening and Nephrotoxicity Assessment on Co-culture Microfluidic Kidney Chip. *Scientific Reports*. 2020;10(1):6568-. doi:10.1038/s41598-020-63096-3
9. Zhu H, Fohlerová Z, Pekárek J, Basova E, Neužil P. Recent advances in lab-on-a-chip technologies for viral diagnosis. *Biosensors & Bioelectronics.* 2020;153:112041-112041. doi:10.1016/j.bios.2020.112041
10. Wu J, Dong M, Rigatto C, Liu Y, Lin F. Lab-on-chip technology for chronic disease diagnosis. *NPJ digital medicine.* 2018;1(1):7-7. doi:10.1038/s41746-017-0014-0
11. Gnecco JS, Pensabene V, Li DJ, et al. Compartmentalized Culture of Perivascular Stroma and Endothelial Cells in a Microfluidic Model of the Human Endometrium. *Annals of Biomedical Engineering.* 2017;45(7):1758-1769. doi:10.1007/s10439-017-1797-5
12. Richardson L, Gnecco J, Ding T, et al. Fetal Membrane Organ-On-Chip: An Innovative Approach to Study Cellular Interactions. *Reproductive Sciences (Thousand Oaks, Calif).* 2020;27(8):1562-1569. doi:10.1007/s43032-020-00184-9
13. Lieber CA, Mahadevan-Jansen A. Automated Method for Subtraction of Fluorescence from Biological Raman Spectra. *Applied Spectroscopy.* 2003;57(11):1363-1367. doi:10.1366/000370203322554518
14. Movasaghi Z, Rehman S, Rehman IU. Raman Spectroscopy of Biological Tissues. *Applied Spectroscopy Reviews*. 2007;42(5):493-541. doi:10.1080/05704920701551530
15. Bergholt MS, Zheng W, Lin K, et al. Characterizing variability in in vivo Raman spectra of different anatomical locations in the upper gastrointestinal tract toward cancer detection. *Journal of Biomedical Optics.* 2011;16(3):037003-037003. doi:10.1117/1.3556723

16. Meng F, Lowell CA. Lipopolysaccharide (LPS)-induced macrophage activation and signal transduction in the absence of Src-family kinases Hck, Fgr, and Lyn. *J Exp Med*. 1997;185(9):1661-1670. doi:10.1084/jem.185.9.1661
17. Yoshida I, Ishida K, Yoshikawa H, et al. In vivo profiling of 2,3,7,8-tetrachlorodibenzo-p-dioxin–induced estrogenic/anti-estrogenic effects in female estrogen-responsive reporter transgenic mice. *Journal of Hazardous Materials*. 2020;385:121526. doi:10.1016/j.jhazmat.2019.121526
18. Li X, Li N, Han Y, Rao K, Ji X, Ma M. 2,3,7,8-Tetrachlorodibenzo-p-dioxin (TCDD)-induced suppression of immunity in THP-1-derived macrophages and the possible mechanisms. *Environmental Pollution (1987).* 2021;287:117302-117302. doi:10.1016/j.envpol.2021.117302
19. Iba Y, Harada T, Horie S, Deura I, Iwabe T, Terakawa N. Lipopolysaccharide-promoted proliferation of endometriotic stromal cells via induction of tumor necrosis factor α and interleukin-8 expression. *Fertility and Sterility.* 2004;82:1036-1042. doi:10.1016/j.fertnstert.2004.04.038
20. Osteen KG, Hill GA, Hargrove JT, Gorstein F. Development of a method to isolate and culture highly purified populations of stromal and epithelial cells from human endometrial biopsy specimens. *Fertil Steril*. 1989;52(6):965-972. doi:10.1016/s0015-0282(16)53160-4

# *CHAPTER III: CONCLUSIONS AND FUTURE DIRECTIONS*

As advancements in healthcare continue to be developed and implemented throughout the world, fewer people will succumb to infectious diseases. The dominant medical focus globally will shift from communicable diseases, such as malaria, diarrheal diseases, and lower respiratory infections, to non-communicable diseases, such as cancer, cardiovascular diseases, and endometriosis.[1] The latter have already become the focal point of many research efforts in developed nations, but increased incidence of non-communicable diseases in low- and middle-income countries beckons for the development of more effective and revolutionary treatment and diagnostic approaches. Recent data corroborates this claim. Emergency hospitalizations for endometriosis-related cases have steadily increased since 2011.[2] Furthermore, on average in the United States, women endure the disease for ten years before being properly diagnosed.[3] It is evident that inadequate diagnostic capabilities and unreliable biomarkers for endometriosis are resulting in delayed diagnoses and medical treatments. Given the deleterious nature and progressive severity of endometriosis, there is a pressing need for novel diagnostic approaches to effectively detect its presence in patients sooner in order to mitigate the number of emergency procedures and improve patient health outcomes.

The results of this study highlight the potential of Raman spectroscopy-based measurements to significantly improve current diagnostic capabilities for endometriosis. Raman spectroscopy coupled with the surface plasmon resonance effect enabled the detection of biochemical changes induced in the *in vitro* cellular secretions of murine and human endometriosis models. The distinct spectral differences between the cellular secretions of endometriotic (i.e., TCDD-exposed) and non-endometriotic (i.e., control and LPS- inflamed) cells indicate the sensitivity of Raman measurements to identify modulations in tissue expression

at the biomolecular level. Such findings will provide insight into the biochemical signature of endometriosis and prove invaluable to efforts to improve diagnostics.

Despite this study's promising direction, further research is needed. The immediate next steps of this work are to perform linear discriminant analysis (LDA) and mass spectrometry to confirm the significance of the spectral peaks and definitively assess the composition of the toxin-exposed samples. Additionally, a larger sample size would provide greater statistical power further substantiating the conclusions of this study. Furthermore, future works will utilize plasmonic materials, such as gold and/or silver nanoparticles, as well as substrates with minimal background Raman interference, such as calcium fluoride, quartz, or magnesium fluoride, to augment signal-to-noise ratio (i.e., surface-enhanced Raman spectroscopy).[4,5] Eventually, we seek to integrate Raman spectroscopy-based measurements with the endometrial organ-on-a-chip models developed by the Bruner-Tran and Osteen Labs for more physiologically accurate results and insight into the progression of endometriosis.[6,7]

In future endeavors, translational research will be conducted using a portable Raman spectrometer. Unlike the bulky inVia$^{TM}$ Renishaw, the portable spectrometers enable mobile Raman readings which is more amenable to clinical and workflow implementation. Although there are several viable portable Raman spectrophotometers, our initial device prototypes have centered around the Wasatch Photonics 633 Raman Spectrometer Series system due to its versatility and easy setup process. This system uses a 633nm excitation laser with a laser spot of

60μm and working distance of 22mm.[8] We have designed a preliminary 3D-printed glass slide holder using SOLIDWORKS™ that is compatible with the portable system (Fig. 16-17).

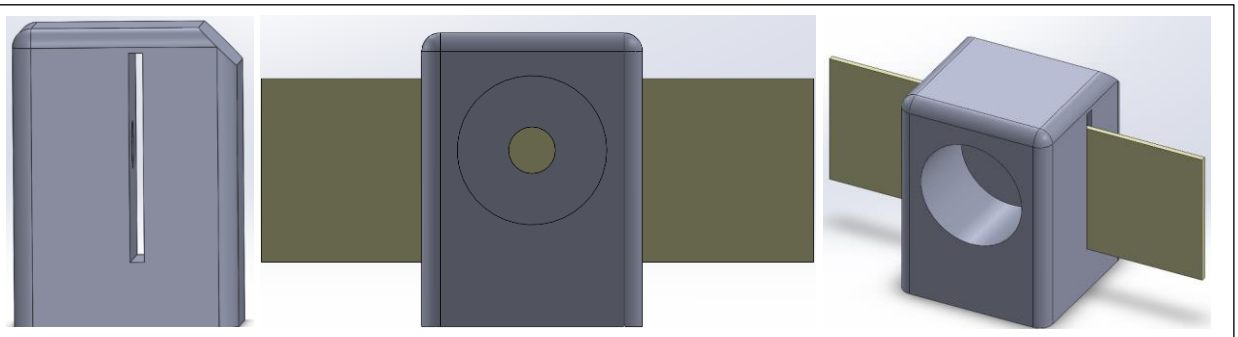

**Figure 16.** CAD model for glass slide holder.

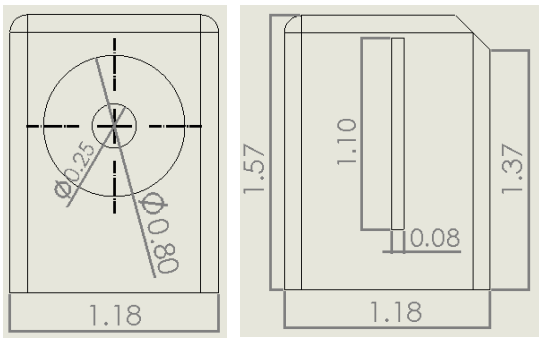


**Figure 17.** Glass slide holder dimensions.

The goal of the slide holder is to allow for repeatable Raman measurements of dried droplets on aluminum foil-wrapped glass slides. The Raman readings from the Wasatch Photonics 633 Raman Spectrometer Series system will be compared to those of the inVia™ Renishaw (i.e. variability, spectral intensity, ease of peak detection, SNR, etc.) in order to evaluate the ability of the portable system to serve as effective replacement for the Renishaw system in analyzing biological specimen.

A few limitations were also present in this study. Aside from the limited sample size, there was a lack of droplet characterization (i.e., imaging, size quantification, droplet variation, and average evaporation time). Furthermore, the background signal emitted from the aluminum

foil (i.e., 1250-1410cm$^{-1}$ region) interfered with analysis within that region. As previously mentioned, a substrate with less background noise would prove beneficial and allow for a more comprehensive spectral analysis within this region.

Overall, this research underlined the potential of Raman spectroscopy to non-invasively detect biochemical changes in endometriosis models. Spectral differences correlated to altered expression levels of amino acids/proteins, lipids, carbohydrates, and nucleic acids. Given the lack of current biomarkers, this study provides essential insight into the biochemical signature of TCDD-induced endometriosis.

## References


1. Bigna JJ, Noubiap JJ. The rising burden of non-communicable diseases in sub-Saharan Africa. *The Lancet Global Health.* 2019;7(10):e1295-e1296. doi:10.1016/S2214-109X(19)30370-5
2. Le Moal J, Goria S, Chesneau J, et al. Increasing incidence and spatial hotspots of hospitalized endometriosis in France from 2011 to 2017. Scientific reports. 2022;12(1):6966-6966. doi:10.1038/s41598-022-11017-x
3. Mayo Clinic Staff. Endometriosis. *Mayo Clinic.* Published July 24, 2018. https://www.mayoclinic.org/diseases-conditions/endometriosis/symptoms-causes/syc-20354656
4. Koya AN, Zhu X, Ohannesian N, et al. Nanoporous Metals: From Plasmonic Properties to Applications in Enhanced Spectroscopy and Photocatalysis. *ACS Nano*. 2021;15(4):6038-6060. doi:10.1021/acsnano.0c10945

5. Kerr LT, Byrne HJ, Hennelly BM. Optimal choice of sample substrate and laser wavelength for Raman spectroscopic analysis of biological specimen. *Analytical Methods.* 2015;7(12):541-552. doi:10.1039/c5ay00327j
6. Gnecco JS, Pensabene V, Li DJ, et al. Compartmentalized Culture of Perivascular Stroma and Endothelial Cells in a Microfluidic Model of the Human Endometrium. *Annals of Biomedical Engineering.* 2017;45(7):1758-1769. doi:10.1007/s10439-017-1797-5
7. Richardson L, Gnecco J, Ding T, et al. Fetal Membrane Organ-On-Chip: An Innovative Approach to Study Cellular Interactions. *Reproductive Sciences (Thousand Oaks, Calif).* 2020;27(8):1562-1569. doi:10.1007/s43032-020-00184-9
8. Wasatch Photonics. WP 633 Raman Spectrometer - Wasatch Photonics. *Wasatch Photonics*. Published April 6, 2023. https://wasatchphotonics.com/product/wp-633-sr-ic-raman-spectrometer/